

Active Sites of Cu/ZnO-Based Catalysts for CO₂ Hydrogenation to Methanol: Part I

Methanol synthesis, catalyst development and role of active sites

Mustafa Al Salmi*

Petroleum Development Oman, PO Box 81,
Muscat, Oman

Email: *Mustafa.MMA.Alsalmi@pdo.co.om

PEER REVIEWED

Received 15th December 2023; Revised 10th March 2024; Accepted 14th March 2024; Online 14th March 2024

Heterogeneous Cu/ZnO-based catalysts are widely used for CO₂ hydrogenation to methanol, but limitations remain for industrial applications. These include achieving high methanol selectivity and conversion and mitigating deactivation by water poisoning. Part I of this review explores the role of active sites on Cu/ZnO-based catalysts in CO₂ conversion. The synergistic interaction between copper and zinc oxide is emphasised, particularly regarding interfacial effects on carbon monoxide activation and formate formation. The discussion covers theoretical and experimental perspectives on active site characteristics, including defects, vacancies, steps and strain. Additionally, the review explores the connection between Cu/ZnO-based catalysts properties and methanol synthesis activity.

Keywords

Cu/ZnO catalysts, CO₂ hydrogenation, methanol, active sites, structure characterisation

1. Introduction

Carbon dioxide is a greenhouse gas emitted from the combustion of fossil fuels, which include natural

gas, oil, biomass and coal (1, 2). Annually, 35 billion metric tonnes of CO₂ are emitted globally, which amounts to about 76% of total global greenhouse emissions (1, 2). The CO₂ in the atmosphere can trap, adsorb and radiate heat, which can lead to rises in sea levels and changes in weather patterns (3). This, as a result, accelerates fresh water shortages and ocean acidification (4). It is clear from recent studies that the CO₂ level is increasing by 2.2 ppm per year and by 2025, the CO₂ level in the atmosphere will surpass 437 ppm, up from 411 ppm in 2019 (5). Therefore, developing CO₂ reduction technologies is necessary in order to minimise the CO₂ concentration level to the standard level by either storing CO₂ or converting CO₂ into methanol (5, 6). This requires highly reactive and selective heterogeneous catalysts to convert large amounts of CO₂ into valuable products like methanol in a short synthesising time (7). In this regard, recent studies have reported that Cu/ZnO/Al₂O₃ catalysts can be used to convert CO₂ to methanol (from a mixture of carbon monoxide, CO₂ and hydrogen, known as synthesis gas or syngas). We note that methanol can be also made from a mixture of CO₂ and hydrogen by using Cu/ZnO-based catalysts (8). However, there are still several technical challenges for those catalysts, which include the requirement of high operating pressure, low methanol selectivity and conversion (8, 9).

1.1. Methanol Synthesis

Methanol is a versatile compound with a wide range of applications. It serves as a valuable source of high-density hydrogen and is utilised as a fuel in fuel cells, offering a clean and efficient energy source for various applications. (2, 9–11). Methanol's diverse applications extend beyond its

role as a fuel source. It is commonly employed as an antifreeze agent (12), a denaturing additive for ethanol and a key component in the chemical industry for the manufacture of polymers, paints, resins and rubbers (13, 14). Given its extensive applications, understanding the intricacies of methanol synthesis is of paramount importance. In the following section, we present a comprehensive discussion on the latest advancements in methanol synthesis research (12, 14).

Methanol can be produced from petroleum feed stocks (synthesis gas) like methane and non-petroleum feedstocks such as coal and biomass. Methanol is conventionally synthesised through the hydrogenation of carbon monoxide and CO₂ and the reverse water–gas shift (RWGS) reaction at low temperature and high pressure, as shown in Equations (i)–(iii), respectively (2, 8–11, 15):



It has been reported that there are two CO₂ hydrogenation pathways using copper-based catalysts. The first pathway includes producing the carbon monoxide through RWGS, which is then used as an intermediate to produce methanol *via* carboxyl (COOH) (RWGS+CO-Hydrogenation pathway) (see **Figure 1**) (16–18). The second pathway includes production of methanol through CO₂ hydrogenation by forming formate (*HCOO) (* denotes surface adsorbed species with the lowest energy barriers) intermediate as well as aldehyde HCO and formaldehyde H₂CO (formate pathway) (see **Figure 1**) (17, 19–21). Generally, the formate pathway is considered more active and selective for direct CO₂ conversion to methanol compared to the RWGS+CO-Hydrogenation pathway. This is because the formate pathway efficiently utilises CO₂ as a reactant, while the RWGS pathway produces carbon monoxide as an intermediate, requiring a separate hydrogenation step for methanol formation. (17, 19). However, the active sites still play a major role in methanol production as there are many facets within the metal/oxide catalysts, which mean multiple interfaces that control the rate of the steps, not just the binding energies.

The process of methanol synthesis from CO₂ and hydrogen is an exothermic reaction, which means that it is thermodynamically limited at high temperatures, but kinetically, the methanol synthesis is limited at low temperatures (15, 22). As the first and second reactions above are exothermic and reversible, the

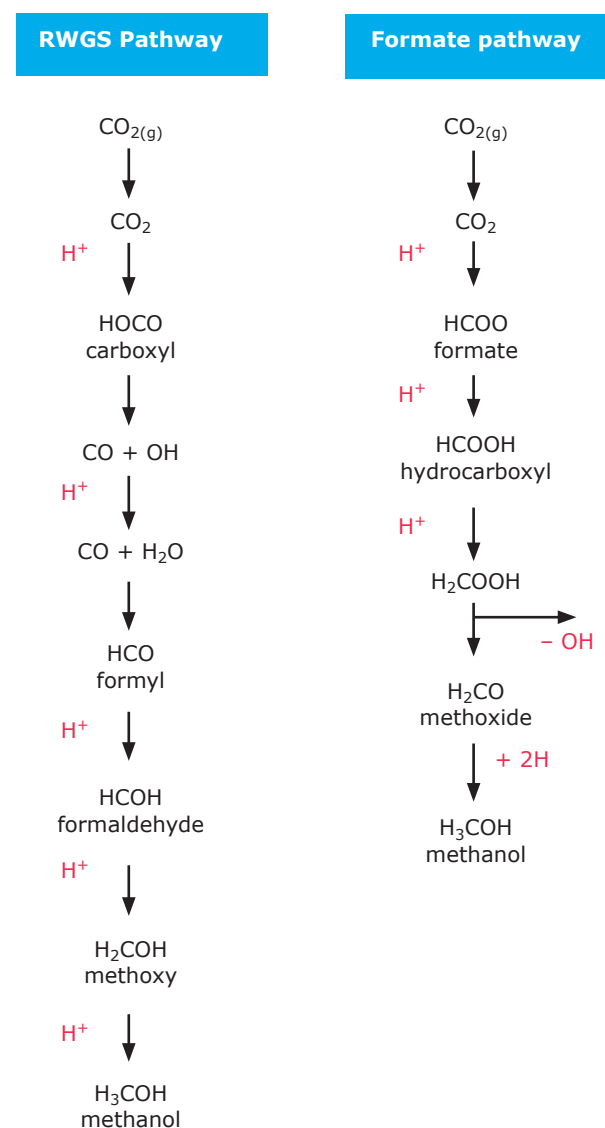


Fig. 1. Diagram showing the reaction network for RWGS and formate pathways of methanol synthesis from CO₂ hydrogenation over copper-based catalysts

conversion of carbon monoxide or CO₂ into methanol is a function of temperature and pressure at equilibrium (13). Hence, Kyrimis *et al.* found that the heat of the reaction associated with CO₂ conversion into methanol and water is -49 kJ kmol^{-1} (23), which is lower than the heat of the reaction associated with carbon monoxide conversion to methanol, with $-90.64 \text{ kJ kmol}^{-1}$ (23–25). This occurs due to the water–gas reaction that associated with CO₂ conversion into methanol (14). Moreover, it has been also reported that the pressure has a large effect on the equilibrium of both the reactions because as the temperature decreases, the equilibrium constant (k_p) decreases (11, 13).

In methanol production plants, natural gas is pre-treated through a purification system that contains hydro-desulfurisation catalysts to remove hydrogen sulfide because it reduces the activity of the reforming catalyst. Then, the natural gas is heated and mixed within the reforming unit to produce synthesis gas that contains carbon monoxide, CO₂ and hydrogen (13, 26). The synthesis gas can be produced through either steam reforming of methane (Equation (vi)), CO₂ reforming of methane (Equation (v)), partial oxidation of methane (Equation (vi)), or tri-reforming of methane (TRM) processes, as shown in Equations (iv)–(vi) (2, 10):



The main factors that affect the conversion of synthesis gas are the ratio of CO:CO₂ and the concentration of carbon monoxide. A higher CO:CO₂ ratio means more synthesis gas can be converted because it increases the reaction rate and decreases the catalytic deactivation rate. On the other hand, higher concentrations of methane, argon and nitrogen will lower the partial pressure of the active reactant (27). After the synthesis gas is produced, the synthesis gas is cooled, compressed and recirculated before it is converted to crude methanol that contains methanol and traces of other byproducts, which include water and dissolved gas, through a methanol convertor at a pressure of 10 MPa. The refined methanol is obtained through additional distillation to remove water and heavy distillate (27). To overcome these challenges, the identification of active sites and their thermodynamics are the best way to either develop new highly active catalysts or increase the selectivity of the currently used industrial catalysts.

Cu/ZnO catalysts were one of the first heterogeneous catalysts to be used for hydrogenation of CO₂ into methanol, in which the copper is the active phase and zinc oxide is the stabiliser of the reaction intermediates (18). In addition, oxygen vacancy defects in zinc oxide play the role of active sites of zinc oxide which can be filled with one oxygen atom of the dioxomethylene H₂COO intermediate in the formate pathway (18, 28). Furthermore, zinc oxide has the features of enhancing formate dissociation without poisoning the surface of oxygen (28, 29). Additionally, the role of active sites on Cu/ZnO catalysts is increasing the ability of hydrogen dissociation into the atomic H* and COO*

(* denotes surface adsorbed species with the lowest energy barriers). In general, the addition of zinc or zinc oxide can enhance the stabilisation of the HCOOH intermediates *via* direct Zn–O interaction and by activating HCOO *via* hydrogenation (30, 31). Cu/ZnO catalysts are more prone to deactivation by water compared to Cu/ZnO/Al₂O₃. Water is produced as a byproduct during CO₂ hydrogenation to methanol through Cu/ZnO catalysts through a series of intermediate steps, specifically during the hydrogenation of formate (HCOO) to formaldehyde (H₂CO) (see Equation (ii) and **Figure 1**) (2, 10, 15). The substantial water production during CO₂ hydrogenation promotes the sintering and crystallisation of Cu/ZnO catalysts, leading to a decline in catalytic activity and selectivity. This phenomenon results in the formation of undesirable byproducts, including higher alcohols such as ethanol, which diminishes the overall methanol yield (18, 32). The main reason for this deactivation is that water can cause the Cu/ZnO catalyst to sinter, which is the process of the small particles of the catalyst clumping together into larger particles. This reduces the surface area of the catalyst, which makes it less effective at catalysing the reaction. Additionally, water can also cause the Cu/ZnO catalyst to crystallise, which changes the structure of the catalyst and makes it less active (32, 33). As a result, Cu/ZnO catalysts have been largely replaced by more water-resistant catalysts, such as those based on palladium or ruthenium (15, 17). These catalysts are less susceptible to sintering and crystallisation in the presence of water, making them more suitable for industrial CO₂ hydrogenation processes. However, research is ongoing to develop new Cu/ZnO catalysts that are more resistant to water-induced deactivation. If successful, these catalysts could potentially be used in industrial CO₂ hydrogenation processes, as they offer several advantages over other catalyst types, such as lower cost and higher selectivity for methanol production (15, 18, 32).

1.2. Catalyst Development

The first methanol synthesis using syngas that contains CO₂ and at high pressures (250–350 bar) was reported in 1923. In this study, high pressure was used as it thermodynamically favours methanol formation (34, 35). The copper catalyst was the first catalyst that was used for synthesis gas conversion into methanol using a high pressure reactor (25 MPa) (13, 16). However, the high poisoning

rate of copper led to the development of a zinc chromite ($\text{Cr}_2\text{O}_3\text{-ZnO}$) that operated between 573–673 K and at a pressure above 30 MPa (9). While high-pressure methanol conversion processes achieved significant conversion rates, their non-portability and high economic costs hindered their feasibility for large-scale industrial applications. Therefore, iron catalyst was developed, as it was used in Fischer–Tropsch reactions with similar conditions to methanol synthesis (9). However, there are some limitations of using iron catalysts, which includes the requirement of high purity of hydrogen and carbon as well as the low methanol conversion through one pass within the reactor, which requires recycling of synthesis gas multiple times (9). On the other hand, the replacement of zinc oxide with Cu/ZnO catalysts led to a reduction in the required reaction pressure from 20–30 MPa to 5–10 MPa, as well as in reaction temperature from 550 K to 500 K (12, 24). It was reported that copper and zinc oxide alone exhibit insignificant activity (36, 37).

The development of oxides like zinc oxide in terms of modification of the electrical properties was established in 1950s to enhance catalysts' activity *via* radiation like gamma radiation. When zinc oxide is irradiated with gamma radiation, it creates defects in the crystal lattice that can act as electron sources and sinks (38). Barry and Roberts were the first who found that radiation can increase the rate of formation of methanol over irradiated zinc oxide, which can activate the zinc oxide at temperatures above 623 K for carbon monoxide and hydrogen conversion into methanol. Since the reaction equilibrium is favourable at low temperatures, they found that the required temperature to induce the reaction is about 533 K by using a cobalt 60 source, with 20% of the electrons that are induced by irradiation being effective in promoting catalytic reactions (38). This occurs due to the direct contribution of electrons that are produced by radiation, as both hydrogen and carbon monoxide are absorbed as ions so that energetic electrons may be exposed to influence adsorption and reaction rates (38).

The methanol production increased dramatically after the development of the Cu–Zn–Cr catalyst by Imperial Chemical Industries (ICI) in 1963, which could be operated at low pressures (3 MPa) (compared to preceding technologies) (39) and temperatures (473–573 K) (see **Figure 2**) (9, 39). Since 1974, Cu/ZnO/Al₂O₃ is the most common catalyst that has been used for methanol synthesis from syngas derived from coal or natural gas, due

to its high activity and selectivity at 493–573 K and an moderate pressure (5–10 MPa) (13, 17, 30, 34, 40, 41). The dominating factor for catalyst development is determined by the ability of its surface to stabilise the desired intermediate, which controls the yield of CO₂ adsorption and conversion into methanol (15). A graphical summary of the development of key catalysts since the 1920s is presented in **Figure 2**.

VOSviewer visualisation software (version 1.6.18, USA, 2022) (42) was used to analyse the keywords in the available literature and patents published from 1930 to 2020 (**Figure 3**) to elucidate the research and development and the direction of research in the field of CO₂ conversion to methanol using Cu/ZnO-based catalysts. The top research directions in this area are surface area, synthesis, Cu/ZnO catalyst and CO₂ hydrogenation. A strong connection was found between the keywords 'surface area' and 'methanol synthesis catalyst' between 2010 and 2020, indicating high research interest in investigating the role of catalyst surface area. Furthermore, the direction of research in this field is moving towards solving the problem of increasing the catalyst activity of Cu/ZnO catalysts. Dimethyl ether (DME) was widely studied *via* methanol dehydration through Cu/ZnO catalysts between 2000 and 2010, but this research decreased significantly after 2010. This decrease is likely related to the generation of water during the process of CO₂ hydrogenation to methanol, which can induce copper sintering of the catalyst as well as coke formation (33). Interestingly, the keyword 'active site' was not found in the analysis, indicating that relatively few papers have been published on the identification and numbering of active sites on Cu/ZnO catalysts. Therefore, more in-depth studies in this area are needed.

The majority of research on CO₂ hydrogenation to methanol conversion focuses on three main areas. In the first area, the working mechanisms of the Cu/ZnO/Al₂O₃ catalyst on model systems are

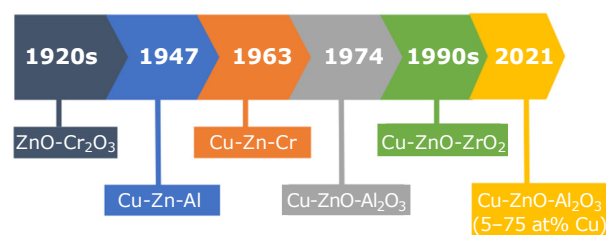


Fig. 2. A timeline of Cu/ZnO development for CO₂ hydrogenation into methanol

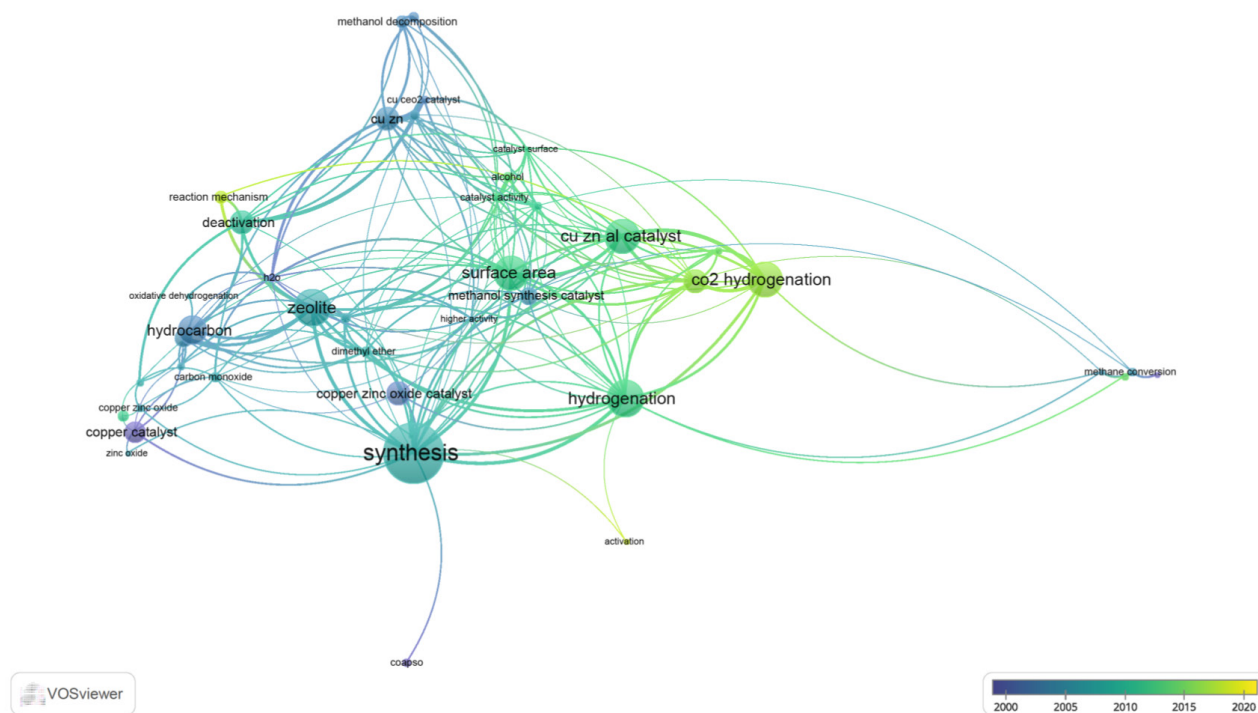


Fig. 3. The keyword network visualisation for CO₂ conversion to methanol on the Cu/ZnO catalyst by using VOSviewer based on data from Web of Science™

reported (43–46). The second one is targeted on the experimental development of higher-efficiency methanol catalysts (46–49). The third area focuses on the increase in the catalytic stability of the catalyst through the investigation of the active phase of the catalyst, including the synergistic interaction between Cu/ZnO and copper-zinc alloy (50–52). In general, attention has been placed on the selectivity of Cu/ZnO catalysts, that depends on the morphology of the catalyst and activity, which depends on the interaction at the interface between copper and zinc oxide (48, 53, 54). However, the catalyst development must also consider the parameters under reaction conditions that affect the catalyst selectivity, such as reconstruction of active sites, oxidation and reduction of sites. Furthermore, the state of the Cu/ZnO-based catalyst is a major challenge in catalytic development, as it depends on the experimental conditions such as partial pressure, sample preparation and temperature, which all have implications for the nature of the active sites (55, 56).

This review article aims to provide a comprehensive understanding of the role of active sites in Cu/ZnO-based catalysts for efficient CO₂ hydrogenation to methanol. By exploring the intricate mechanisms of CO₂ conversion to carbon monoxide *via* the RWGS

pathway and CO₂ conversion into methanol *via* the formate pathway, the review sheds light on the catalytic intricacies involved in this transformative process. The review delves into the electronic properties and bulk structure of Cu/ZnO catalysts, highlighting the influence of catalyst microstructure on methanol synthesis activity. It also examines various modifications of Cu/ZnO catalysts, including the impact of sample preparation methods, the role of alumina in enhancing selectivity and the effects of precipitation temperature and pH during catalyst synthesis. The review also discusses multiscale modelling approaches for characterising active sites, providing a deeper understanding of the underlying catalytic processes. By addressing the deactivation mechanisms of Cu/ZnO-based catalysts and identifying remaining challenges and future research directions, the review paves the way for further advancements in this promising field.

2. Role of Active Sites on Cu/ZnO Catalyst

The Cu/ZnO system is a non-uniform heterogeneous catalyst that comprises a combination of copper nanoparticles dispersed on a zinc oxide support (30, 43). This arrangement creates a heterogeneous surface with a variety of active sites, including

copper steps, zinc atoms, bulk defects and oxygen vacancies. These diverse active sites play crucial roles in the adsorption, activation and conversion of reactants during catalytic reactions (30, 44, 46, 47).

The copper steps, which are essentially edges or boundaries between copper crystal facets, provide highly reactive sites for CO₂ adsorption and activation (30, 31, 44). Bulk defects and oxygen vacancies within the zinc oxide support can also contribute to the catalytic activity by providing additional adsorption sites and altering the electronic structure of the catalyst surface. These defects can facilitate the transfer of electrons between copper and zinc oxide, enhancing the catalyst's ability to activate reactants (30, 31, 43, 56, 57).

The active site in a Cu/ZnO catalyst is associated with partially and completely reduced copper and with the interaction of fully or partially reduced zinc oxide (57). The main active sites of Cu/ZnO catalysts are the metallic copper, including Cu⁰ and Cu⁺ species and because of this, the activity of Cu/ZnO catalysts is directly proportional to the copper surface area (58–60). However, the majority of the contribution of active sites comes from the non-ideal nature of copper atoms, which have micro-strains in the copper phase (32, 44). As a result, the strain in the copper metal phase is the main correlated source for the turnover frequency of methanol synthesis (36). The main sources of strain in Cu/ZnO catalysis are structural defects from copper in zinc oxide, which cause epitaxial growth orientation in zinc oxide, leading to lattice defects from the copper surface phase modification that gives rise to the catalytic activity of the Cu/ZnO catalysts (32). Furthermore, Günter *et al.* concluded that the phase composition of hydroxycarbonate precursor (like zincian malachite) plays a key role in determining the formation and characteristics of the active copper and zinc oxide phases in the final Cu/ZnO catalyst for methanol synthesis (36). Their findings suggest that the specific structure and properties of the precursor influence the development of the active catalyst phases, ultimately impacting its activity and selectivity (36).

The Cu–ZnO interface plays a pivotal role in the catalytic activity of Cu/ZnO catalysts due to the synergistic interplay between copper and zinc oxide at the atomic level. While copper is primarily responsible for the activation and conversion of reactants, zinc oxide serves as a stabiliser for reaction intermediates, enhancing the overall

efficiency of the catalytic process (15, 18). There are many theories that explain the nature of intermolecular interaction between copper and zinc oxide and the corresponding role of active sites. The first theory was reported by Klier *et al.*, who stated that copper is incorporated on interstitial and substitutional sites in the zinc oxide phase with three possible valence states (Cu⁰, Cu⁺ and Cu²⁺) (61). Another theory was proposed by Chinchén *et al.*, who concluded that only copper carries catalytic activity and zinc oxide merely stabilises the copper surface area (62). This theory assumed that the only role of zinc oxide is as an inert support and as a promoter for the system. In addition, Chinchén *et al.* found a linear relationship between the copper specific surface area and catalytic area (62). On the other hand, Burch *et al.* proposed that zinc oxide is not only inert support, but it also serves as a hydrogen reservoir (63), i.e., the hydrogen is adsorbed on it from the spillover of hydrogen atoms during the hydrogenation of formate adsorbed on the copper (27, 36).

Looking closely at the copper low-index surfaces, it was experimentally reported that Cu(110) catalysts are catalytically more active for CO₂ dissociation as compared to Cu(111) and Cu(100) surfaces (15, 28, 64–66). The Cu(110) surface exhibits a unique arrangement of copper atoms, with a higher density of step edges and undercoordinated sites compared to Cu(111) and Cu(100) surfaces. These step edges and undercoordinated sites provide more reactive sites for CO₂ adsorption and activation, facilitating the dissociation of CO₂ into carbon monoxide and oxygen (15, 28, 64–67). Previously, it has been reported that formate species were most stable on the Cu(110) surface (67, 68). The enhanced stability of formate species on the Cu(110) surface compared to Cu(111) and Cu(100) surfaces can be explained by analysing the electronic structure and orbital interactions between formate and the copper surfaces (67, 68). On the Cu(111) surface, the d-orbitals of the surface copper atoms are fully occupied and strongly overlap, forming stable chemical bonds within the copper lattice. This leaves limited availability for interactions with the formate species, resulting in weaker adsorption and stability. In contrast, on the Cu(100) and Cu(110) surfaces, the d-orbitals in the bonding region are more dispersed, creating a favourable environment for hybridisation between the oxygen (s, p) orbitals of the formate species and the surface copper (s, p, d) orbitals (67, 68). This hybridisation leads to stronger bonding and enhanced stability of formate on these surfaces. The Cu(110) surface,

in particular, exhibits a unique arrangement of copper atoms with a higher density of step edges and undercoordinated sites (67, 68). These sites provide additional opportunities for orbital overlap and hybridisation with formate, further stabilising its adsorption on the Cu(110) surface. Therefore, the combination of dispersed d-orbitals and the presence of step edges and undercoordinated sites on the Cu(110) surface facilitates stronger hybridisation between formate and copper, resulting in enhanced stability of formate species compared to Cu(111) and Cu(100) surfaces (67, 68). The enhanced stability of formate species on the Cu(110) surface compared to Cu(111) and Cu(100) surfaces can be attributed to the specific d-orbitals involved in the chemical bonding between the formate and the copper surfaces. On the Cu(110) surface, the d_{yz} and d_{xz} orbitals of the surface copper atoms play a dominant role in the bonding with formate. These orbitals are energetically favourable for hybridisation with the oxygen (s, p) orbitals of formate, leading to strong bonding and enhanced stability. In contrast, on the Cu(100) surface, the $d_{x^2-y^2}$ and d_{z^2} orbitals are primarily involved in the bonding with the formate. However, these orbitals are higher in energy due to the octahedral-like crystal field splitting, resulting in weaker bonding and less stable formate adsorption compared to the Cu(110) surface. The Cu(111) surface exhibits the lowest catalytic activity for methanol synthesis due to the limited availability of active sites for formate adsorption and activation. This is reflected in the lower turnover frequency (TOF) of $0.006 \text{ M}^{-1} \text{ s}^{-1}$ for Cu(111) compared to $0.032 \text{ M}^{-1} \text{ s}^{-1}$ for Cu(110) (30, 67, 69, 70). Therefore, the specific d-orbitals involved in the chemical bonding between formate and copper surfaces play a crucial role in determining the stability of formate species and the overall catalytic activity for methanol synthesis. The Cu(110) surface, with its favourable d_{yz} and d_{xz} orbitals, provides the most stable adsorption sites for formate and exhibits the highest catalytic activity among the three copper surfaces (30, 67, 69, 70).

The catalytic performance of Cu/ZnO catalysts for methanol synthesis is significantly influenced by the nature of active sites, particularly the d-band centre of copper and defect states in zinc oxide. Additionally, the size of copper and zinc oxide crystallites plays a crucial role in determining the strength of CO₂ adsorption, which is a critical step in the methanol synthesis pathway (15, 30). The d-band centre of copper represents the energy level of the d-orbitals in copper, which are involved

in the adsorption and activation of reactants. A lower d-band centre indicates a higher energy level of d-orbitals, leading to stronger interactions with reactants and enhanced catalytic activity. Defect states in zinc oxide, such as oxygen vacancies, can also contribute to the catalytic activity by providing additional adsorption sites and modifying the electronic properties of the catalyst surface (18, 28). These defect states can facilitate electron transfer between copper and zinc oxide, enhancing the catalyst's ability to activate CO₂ (46, 47). The size of copper and zinc oxide crystallites also plays a crucial role in determining the strength of CO₂ adsorption. Smaller crystallites provide a higher density of active sites and a larger surface area for CO₂ adsorption, leading to stronger interactions and enhanced catalytic activity (15, 71). The deposition of zinc oxide on the Cu(111) surface has been shown to increase the reaction rates of methanol synthesis by 5–18 times compared to the Cu(110) surface (30). This enhancement is attributed to the higher number of reactive surfaces and a higher concentration of corner and edge atoms on Cu(111) compared to Cu(110). Corner and edge atoms on copper surfaces provide more reactive sites for CO₂ adsorption and activation due to their unique electronic structure and coordination environment. These sites can effectively bind and activate CO₂, promoting its conversion to methanol. Therefore, the combination of a favourable d-band centre of copper, defect states in zinc oxide and an optimal crystallite size contributes to the enhanced catalytic performance of Cu/ZnO catalysts for methanol synthesis. The deposition of zinc oxide on Cu(111) further improves the activity by increasing the number of reactive surfaces and corner or edge atoms, facilitating CO₂ adsorption and activation (28, 31).

Theoretical modelling techniques, such as density functional theory (DFT) and kinetic Monte Carlo (kMC) simulations, have provided valuable insights into the role of active sites on Cu/ZnO catalysts for methanol synthesis. These studies have revealed that the presence of zinc oxide and the formation of copper–zinc active sites play crucial roles in enhancing the catalytic activity. DFT calculations have shown that methanol synthesis on the Cu(111) surface in the presence of water is energetically more favourable with COOH as the intermediate compared to formate species (28, 31). This is because zinc oxide acts as a stabiliser for the intermediates, promoting formate dissociation without poisoning the surface (28, 29). Furthermore, the formation of zinc-copper

dispersed on zinc sites has been associated with high methanol synthesis rates. This dispersion effect leads to the creation of copper–zinc active sites, which exhibit enhanced catalytic activity compared to pure copper or zinc oxide surfaces (28, 29, 31). However, studies have also indicated that ZnCu(111) surfaces are not stable due to the transformation of zinc into zinc oxide and the growth of copper on the oxygen-terminated (000 $\bar{1}$) face of zinc oxide. These processes can hinder CO₂ adsorption and reduce the catalytic activity (20, 30, 72–74). Thermodynamically, CO₂ has a large ionisation potential and a small electron affinity, indicating its ability to accept electrons from catalyst sites. The primary role of active sites is to inject electrons into the antibonding orbital of CO₂, promoting its activation and conversion to methanol (18). The hydrogen feed acts as a reducing agent, providing the necessary electrons for CO₂ reduction and methanol formation. The synergistic interplay between copper and zinc oxide, along with the presence of hydrogen, facilitates the overall methanol synthesis process (18).

In terms of the theoretical studies using the kMC method, Pavlišić *et al.* studied the surface coverage of the Cu/ZnO catalyst as a function of time (75). They found that temperature and pressure are dependent on surface intermediate species of H, formate (HCOO) and methoxy (CH₃O), as illustrated in **Figure 4**. The surface coverage is inversely proportional to temperature and directly proportional to pressure, i.e., the interaction of these intermediates is strongly dependent on pressure and temperature (see **Figure 4**).

However, a significant increase in surface coverage of methoxy was found in relation with temperature because methoxy intermediate concentration is strongly dependent on reaction rate. At low pressure (1 bar), all the intermediate coverages are low and increases with pressure. This means that the H, HCOO and CH₃O intermediates are the most abundant surface species with significant dependence on temperature and pressure of the surface species composition.

3. Reaction Mechanism of CO₂ Conversion to Carbon Monoxide through RWGS Pathway

There are two proposed mechanisms of the RWGS reaction over the Cu/ZnO catalyst. The first is the surface formate decomposition mechanism and the second is the surface redox mechanism (76–78). The rate determining step in the RWGS reaction is the dissociation of CO₂ (76). The carbon monoxide formation from the RWGS reaction is significantly influenced by the interfacial area between the zinc oxide and copper. This is because copper sites exhibit a high affinity for dissociating hydrogen molecules, generating reactive atomic hydrogen. This atomic hydrogen then spills over onto the zinc oxide surface, where it facilitates the hydrogenation of adsorbed CO₂ molecules, ultimately leading to carbon monoxide formation (15, 23, 79, 80). The RWGS reaction is an endothermic process, necessitating high temperatures for carbon monoxide production. Despite this energy requirement, the RWGS reaction remains economically attractive due to the value

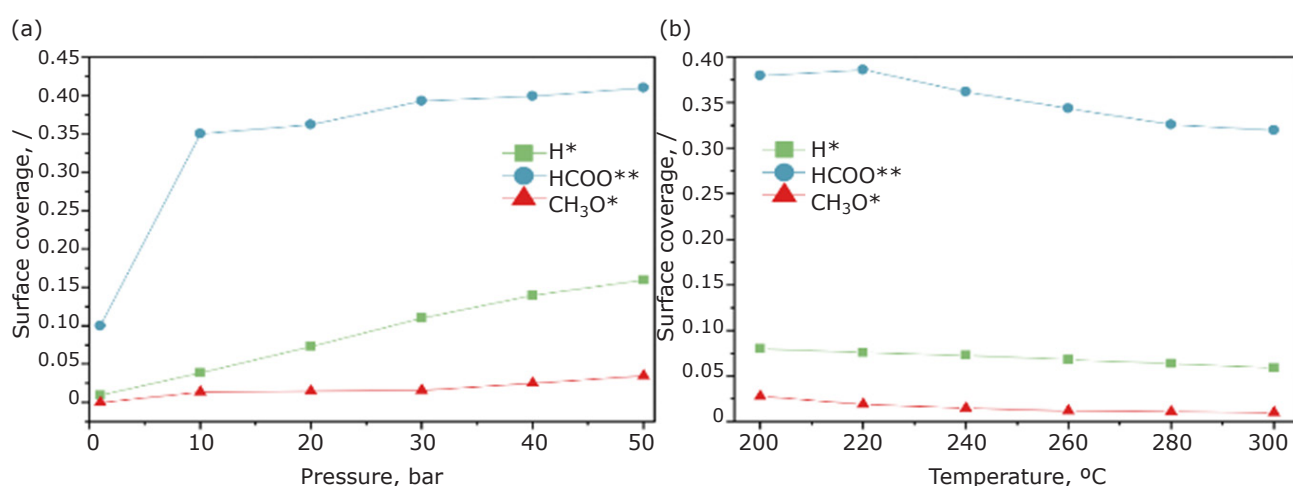


Fig. 4. The relationship between the surface coverage (/) and: (a) pressure (bar); (b) temperature (°C) obtained *via* the kMC method. The * denotes active site on catalytic surface and ** stands for formed intermediate (75). Copyright 2020 Elsevier

of the generated carbon monoxide as a feedstock for the Fischer–Tropsch process (15). Fujita *et al.* used Fourier transform infrared spectroscopy (FTIR) to investigate the mechanism of the RWGS over Cu/ZnO catalysts and they found that two formate species are formed during the CO₂–hydrogen reaction over Cu/ZnO catalysts. In the first formate species, the absorption peaks occur at 1350 cm⁻¹, 1615 cm⁻¹ and 2850 cm⁻¹ and they defined it as formate I and in the second formate II species, the absorption peaks were seen at 2975 cm⁻¹, 2740 cm⁻¹, 2880 cm⁻¹, 1580 cm⁻¹ and 1350 cm⁻¹ (76). In addition, they found that the water is formed *via* hydrogenation of the surface oxygen species of the Cu/ZnO catalyst. Also, they found that, over the Cu/ZnO catalyst, CO₂ dissociates into carbon monoxide and an oxygen atom (O) adsorbed on the surface (76). Furthermore, they found that the surface oxidation and reduction of RWGS take place with CO₂ and hydrogen over the copper surface, as shown in the scheme (see **Figure 5**) (76). As a result, surface cuprous oxide (Cu₂O) is formed *via* dissociation of CO₂ and therefore the rate determining step in RWGS is the oxidation of the copper surface in a Cu/ZnO catalyst with CO₂ (76).

There are many reaction parameters that affect the equilibrium of the RWGS reaction, which include the composition of the syngas feed, pressure, H₂:CO ratio, temperature and space velocity. CO₂ conversion is enhanced at low temperatures with high pressure, which leads to a higher selectivity of methanol production because RWGS is an endothermic reaction. Therefore, RWGS involved carbon monoxide intermediates *via* carboxyl species for hydrogenation in a later stage. Furthermore, the high ratio of H₂:CO₂, with a low concentration of CO₂ and a high concentration of hydrogen, in the fresh feed stream will increase the CO₂ conversion into methanol with low carbon monoxide selectivity

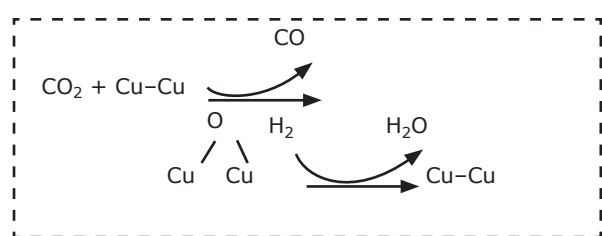


Fig. 5. A schematic diagram illustrates the RWGS reaction process involving the oxidation and reduction of the copper surface through Cu(O) \leftrightarrow Cu(I) with CO₂ and hydrogen (76). Copyright 1991 Elsevier

because it shifts the reaction equilibrium to the product side (17). In RWGS, the strong oxygen affinity of zinc sites makes the surface adsorbed oxygen atom formation more kinetically favourable than hydrogenation to HOCO and competitive with its hydrogenation to HCOO (formate pathway) because the hydrogenation of surface-adsorbed oxygen at the zinc sites to hydroxyl is difficult as surface-adsorbed oxygen species are likely to be stabilised on the surface and lead to the formation of a zinc oxide layer during the CO₂ hydrogenation reaction (15).

Yoshihara and Campbell applied DFT calculations to methanol synthesis through RWGS over Cu(110) catalysts and they found that RWGS formate can proceed through carboxyl intermediates rather than formate intermediates *via* surface redox mechanism. However, most studies support the formate pathway (19, 30, 81–83) for converting CO₂ into methanol rather than RWGS based on DFT calculations. Recently, DFT-based kMC simulation of the WGS reaction on Cu/ZnO catalysts was employed by Yang *et al.* to determine the behaviour and energetics of the reaction (84). They found that the production rate of hydrogen and CO₂ through Cu/ZnO catalysts is strongly dependent on the size and structure of copper (84). In addition, their simulation found that number of both edge and terrace sites of copper is directly proportional to the hydrogen production in the WGS reaction through Cu/ZnO catalysts, which means that those sites are highly active, sensitive and thermodynamically favourable in the WGS reaction for hydrogen and CO₂ production (84–86).

The work will continue in Part II (87) and Part III (88).

Author Contributions

M.A.S.: formal analysis, data curation, writing original draft, software, methodology and validation.

Conflicts of Interest

Author declares no conflict of interest.

References

1. A. Mikhaylov, N. Moiseev, K. Aleshin, T. Burkhardt, *Entrep. Sustain. Issues*, 2020, **7**, (4), 2897
2. H.-K. Lo, C. Copéret, *ChemCatChem*, 2018, **11**, (1), 430
3. L. Al-Ghussain, *Environ. Prog. Sustain. Energy*, 2018, **38**, (1), 13
4. L. Garcia-Cuerva, E. Z. Berglund, A. R. Binder,

- Resour. Conserv. Recycl.*, 2016, **113**, 106
5. P. Friedlingstein, M. W. Jones, M. O'Sullivan, R. M. Andrew, J. Hauck, G. P. Peters, W. Peters, J. Pongratz, S. Sitch, C. Le Quéré, D. C. E. Bakker, J. G. Canadell, P. Ciais, R. B. Jackson, P. Anthoni, L. Barbero, A. Bastos, V. Bastrikov, M. Becker, L. Bopp, E. Buitenhuis, N. Chandra, F. Chevallier, L. P. Chini, K. I. Currie, R. A. Feely, M. Gehlen, D. Gilfillan, T. Gkritzalis, D. S. Goll, N. Gruber, S. Gutekunst, I. Harris, V. Haverd, R. A. Houghton, G. Hurtt, T. Ilyina, A. K. Jain, E. Joetzjer, J. O. Kaplan, E. Kato, K. Klein Goldewijk, J. I. Korsbakken, P. Landschützer, S. K. Lauvset, N. Lefèvre, A. Lenton, S. Lienert, D. Lombardozzi, G. Marland, P. C. McGuire, J. R. Melton, N. Metz, D. R. Munro, J. E. M. S. Nabel, S.-I. Nakaoka, C. Neill, A. M. Omar, T. Ono, A. Peregon, D. Pierrot, B. Poulter, G. Rehder, L. Resplandy, E. Robertson, C. Rödenbeck, R. Séférian, J. Schwinger, N. Smith, P. P. Tans, H. Tian, B. Tilbrook, F. N. Tubiello, G. R. van der Werf, A. J. Wiltshire, S. Zaehle, *Earth Syst. Sci. Data*, 2019, **11**, (4), 1783
 6. K. B. Karnauskas, S. L. Miller, A. C. Schapiro, *GeoHealth*, 2020, **4**, (5), e2019GH000237
 7. J. H. Edwards, *Catal. Today*, 1995, **23**, (1), 59
 8. M. K. Sanghvi, R. R. Judkins, W. Fulkerson, *Sci. Am.*, 1990, **263**, (3), 128
 9. D. Sheldon, *Johnson Matthey Technol. Rev.*, 2017, **61**, (3), 172
 10. Z. Arab Aboosadi, A. H. Jahanmiri, M. R. Rahimpour, *Appl. Energy*, 2011, **88**, (8), 2691
 11. G. H. Graaf, J. G. M. Winkelman, *Ind. Eng. Chem. Res.*, 2016, **55**, (20), 5854
 12. P. Potočník, I. Grabec, M. Šetinc, J. Levec, *Neural Process. Lett.*, 2000, **11**, (3), 219
 13. J. G. van Bennekom, R. H. Venderbosch, J. G. M. Winkelman, E. Wilbers, D. Assink, K. P. J. Lemmens, H. J. Heeres, *Chem. Eng. Sci.*, 2013, **87**, 204
 14. A. Hamnett, *Catal. Today*, 1997, **38**, (4), 445
 15. M. D. Porosoff, B. Yan, J. G. Chen, *Energy Environ. Sci.*, 2016, **9**, (1), 62
 16. C. Murkin, J. Brightling, *Johnson Matthey Technol. Rev.*, 2016, **60**, (4), 263
 17. U. J. Etim, Y. Song, Z. Zhong, *Front. Energy Res.*, 2020, **8**, 545431
 18. Y. Li, S. H. Chan, Q. Sun, *Nanoscale*, 2015, **7**, (19), 8663
 19. S. Kattel, B. Yan, Y. Yang, J. G. Chen, P. Liu, *J. Am. Chem. Soc.*, 2016, **138**, (38), 12440
 20. T. Kubota, I. Hayakawa, H. Mabuse, K. Mori, K. Ushikoshi, T. Watanabe, M. Saito, *Appl. Organomet. Chem.*, 2001, **15**, (2), 121
 21. F. Nestler, A. R. Schütze, M. Ouda, M. J. Hadrich, A. Schaadt, S. Bajohr, T. Kolb, *Chem. Eng. J.*, 2020, **394**, 124881
 22. L. Wang, M. Ghossoub, H. Wang, Y. Shao, W. Sun, A. A. Tountas, T. E. Wood, H. Li, J. Y. Y. Loh, Y. Dong, M. Xia, Y. Li, S. Wang, J. Jia, C. Qiu, C. Qian, N. P. Kherani, L. He, X. Zhang, G. A. Ozin, *Joule*, 2018, **2**, (7), 1369
 23. S. Kyrimis, M. E. Potter, R. Raja, L.-M. Armstrong, *Faraday Discuss.*, 2021, **230**, 100
 24. M. Kuczynski, W. I. Browne, H. J. Fontein, K. R. Westerterp, *Chem. Eng. Process. Process Intensif.*, 1987, **21**, (4), 179
 25. M. Aresta, A. Dibenedetto, *Dalton Trans.*, 2007, (28), 2975
 26. O. Mäyrä, K. Leiviskä, 'Modeling in Methanol Synthesis', in "Methanol: Science and Engineering", eds. A. Basile, F. Dalena, Ch. 17, Elsevier, Amsterdam, The Netherlands, 2018, pp. 475-492
 27. S. C. Kang, K.-W. Jun, Y.-J. Lee, *Energy Fuels*, 2013, **27**, (11), 6377
 28. J. Yoshihara, C. T. Campbell, *J. Catal.*, 1996, **161**, (2), 776
 29. F. Studt, I. Sharafutdinov, F. Abild-Pedersen, C. F. Elkjær, J. S. Hummelshøj, S. Dahl, I. Chorkendorff, J. K. Nørskov, *Nat. Chem.*, 2014, **6**, (4), 320
 30. S. Kattel, P. J. Ramírez, J. G. Chen, J. A. Rodriguez, P. Liu, *Science*, 2017, **355**, (6331), 1296
 31. Y.-F. Zhao, Y. Yang, C. Mims, C. H. F. Peden, J. Li, D. Mei, *J. Catal.*, 2011, **281**, (2), 199
 32. F. Liao, Y. Huang, J. Ge, W. Zheng, K. Tedsree, P. Collier, X. Hong, S. C. Tsang, *Angew. Chem. Int. Ed.*, 2011, **50**, (9), 2162
 33. J. Abu-Dahrieh, D. Rooney, A. Goguet, Y. Saih, *Chem. Eng. J.*, 2012, **203**, 201
 34. A. Bansode, A. Urakawa, *J. Catal.*, 2014, **309**, 66
 35. A. Urakawa, A. Bansode, R. V. Gaikwad, 'Methanol Production Process', *World Patent Appl.* 2017/140800, 24th August, 2017
 36. M. M. Günter, T. Ressler, B. Bems, C. Büscher, T. Genger, O. Hinrichsen, M. Muhler, R. Schlögl, *Catal. Lett.*, 2001, **71**, (1/2), 37
 37. T. Shishido, Y. Yamamoto, H. Morioka, K. Takaki, K. Takehira, *Appl. Catal. A: Gen.*, 2004, **263**, (2), 249
 38. T. I. Barry, R. Roberts, *Nature*, 1959, **184**, (4692), 1061
 39. P. Davies, F. F. Snowdon, G. W. Bridger, D. O. Hughes, P. W. Young, ICI Ltd, 'Water-Gas Conversion and Catalysts Therefor', *British Patent* 1,010,871, 24th November, 1965
 40. H. Yang, P. Gao, C. Zhang, L. Zhong, X. Li, S. Wang, H. Wang, W. Wei, Y. Sun, *Catal. Commun.*, 2016, **84**, 56
 41. K. K. Bando, K. Sayama, H. Kusama, K. Okabe, H. Arakawa, *Appl. Catal. A: Gen.*, 1997, **165**, (1-2), 391
 42. N. J. van Eck, L. Waltman, *Scientometrics*, 2010, **84**, (2), 523

43. L. C. Grabow, M. Mavrikakis, *ACS Catal.*, 2011, **1**, (4), 365
44. M. Behrens, F. Studt, I. Kasatkin, S. Kühl, M. Hävecker, F. Abild-Pedersen, S. Zander, F. Girgsdies, P. Kurr, B.-L. Kniep, M. Tovar, R. W. Fischer, J. K. Nørskov, R. Schlögl, *Science*, 2012, **336**, (6083), 893
45. M. Behrens, S. Zander, P. Kurr, N. Jacobsen, J. Senker, G. Koch, T. Ressler, R. W. Fischer, R. Schlögl, *J. Am. Chem. Soc.*, 2013, **135**, (16), 6061
46. J. Schumann, T. Lunkenbein, A. Tarasov, N. Thomas, R. Schlögl, M. Behrens, *ChemCatChem*, 2014, **6**, (10), 2889
47. E. Frei, A. Schaadt, T. Ludwig, H. Hillebrecht, I. Krossing, *ChemCatChem*, 2014, **6**, (6), 1721
48. M. Kurtz, N. Bauer, C. Büscher, H. Wilmer, O. Hinrichsen, R. Becxker, S. Rabe, K. Merz, M. Driess, R. A. Fischer, M. Muhler, *Catal. Lett.*, 2004, **92**, (1/2), 49
49. J. Xiao, T. Frauenheim, *J. Phys. Chem. Lett.*, 2012, **3**, (18), 2638
50. Y. Choi, K. Futagami, T. Fujitani, J. Nakamura, *Appl. Catal. A: Gen.*, 2001, **208**, (1–2), 163
51. M. Spencer, *Top. Catal.*, 1999, **8**, 259
52. J. Wang, S. Funk, U. Burghaus, *Catal. Lett.*, 2005, **103**, (3–4), 219
53. S. Fujita, M. Usui, H. Ito, N. Takezawa, *J. Catal.*, 1995, **157**, (2), 403
54. G. J. J. Bartley, R. Burch, *Appl. Catal.*, 1988, **43**, (1), 141
55. R. Burch, R. J. Chappell, S. E. Golunski, *Catal. Lett.*, 1988, **1**, (12), 439
56. C. Yang, Z. Ma, N. Zhao, W. Wei, T. Hu, Y. Sun, *Catal. Today*, 2006, **115**, (1–4), 222
57. V. D. B. C. Dasireddy, N. S. Štefančič, B. Likozar, *J. CO₂ Util.*, 2018, **28**, 189
58. W. X. Pan, R. Cao, D. L. Roberts, G. L. Griffin, *J. Catal.*, 1988, **114**, (2), 440
59. S. Natesakhawat, J. W. Lekse, J. P. Baltrus, P. R. Ohodnicki, B. H. Howard, X. Deng, C. Matranga, *ACS Catal.*, 2012, **2**, (8), 1667
60. M. Saito, T. Fujitani, M. Takeuchi, T. Watanabe, *Appl. Catal. A: Gen.*, 1996, **138**, (2), 311
61. K. Klier, *Adv. Catal.*, 1982, **31**, 243
62. G. C. Chinchén, P. J. Denny, D. G. Parker, M. S. Spencer, D. A. Whan, *Appl. Catal.*, 1987, **30**, (2), 333
63. R. Burch, S. E. Golunski, M. S. Spencer, *J. Chem. Soc. Faraday Trans.*, 1990, **86**, (15), 2683
64. I. Nakamura, H. Nakano, T. Fujitani, T. Uchijima, J. Nakamura, *J. Vac. Sci. Technol. A*, 1999, **17**, (4), 1592
65. J. Niu, H. Liu, Y. Jin, B. Fan, W. Qi, J. Ran, *Int. J. Hydrogen Energy*, 2022, **47**, (15), 9183
66. Q. Chen, X. Chen, Q. Ke, *Colloid. Surf. A Physicochem. Eng. Asp.*, 2022, **638**, 128332
67. F. H. P. M. Habraken, G. A. Bootsma, P. Hofmann, S. Hachicha, A. M. Bradshaw, *Surf. Sci.*, 1979, **88**, (2–3), 285
68. A. Chutia, I. P. Silverwood, M. R. Farrow, D. O. Scanlon, P. P. Wells, M. Bowker, S. F. Parker, C. R. A. Catlow, *Surf. Sci.*, 2016, **653**, 45
69. H.-J. Freund, R. P. Messmer, *Surf. Sci.*, 1986, **172**, (1), 1
70. T. Fujitani, J. Nakamura, *Catal. Lett.*, 1998, **56**, 119
71. T. Fujitani, I. Nakamura, T. Uchijima, J. Nakamura, *Surf. Sci.*, 1997, **383**, (2–3), 285
72. M. Behrens, D. Brennecke, F. Girgsdies, S. Kißner, A. Trunschke, N. Nasrudin, S. Zakaria, N. F. Idris, S. B. A. Hamid, B. Kniep, R. Fischer, W. Busser, M. Muhler, R. Schlögl, *Appl. Catal. A: Gen.*, 2011, **392**, (1–2), 93
73. S. Poto, D. V. van Berkel, F. Gallucci, M. F. N. d'Angelo, *Chem. Eng. J.*, 2022, **435**, (2), 134946
74. Y. Slotboom, M. J. Bos, J. Pieper, V. Vrieswijk, B. Likozar, S. R. A. Kersten, D. W. F. Brilman, *Chem. Eng. J.*, 2020, **389**, 124181
75. A. Pavlišič, M. Huš, A. Prašnikar, B. Likozar, *J. Clean. Prod.*, 2020, **275**, 122958
76. S. Fujita, M. Usui, N. Takezawa, *J. Catal.*, 1992, **134**, (1), 220
77. T. van Herwijnen, W. A. de Jong, *J. Catal.*, 1980, **63**, (1), 83
78. D. Grenoble, M. M. Estadt, D. F. Ollis, *J. Catal.*, 1981, **67**, (1), 90
79. C.-S. Chen, W.-H. Cheng, S.-S. Lin, *Appl. Catal. A: Gen.*, 2003, **238**, (1), 55
80. M. Al Salmi, *Johnson Matthey Technol. Rev.*, 2024, **68**, (2), 184
81. J. Wellendorff, K. T. Lundgaard, A. Møgelhøj, V. Petzold, D. D. Landis, J. K. Nørskov, T. Bligaard, K. W. Jacobsen, *Phys. Rev. B*, 2012, **85**, (23), 235149
82. B. Hammer, L. B. Hansen, J. K. Nørskov, *Phys. Rev. B*, 1999, **59**, (11), 7413
83. F. Studt, F. Abild-Pedersen, Q. Wu, A. D. Jensen, B. Temel, J.-D. Grunwaldt, J. K. Nørskov, *J. Catal.*, 2012, **293**, 51
84. L. Yang, A. Karim, J. T. Muckerman, *J. Phys. Chem. C*, 2013, **117**, (7), 3414
85. A. A. Tsyganenko, J. Lamotte, J. Saussey, J. C. Lavalley, *J. Chem. Soc. Faraday Trans. 1 Phys. Chem. Condens. Phases*, 1989, **85**, (8), 2397
86. M. Huš, D. Kopač, B. Likozar, *ACS Catal.*, 2019, **9**, (1), 105
87. M. Al Salmi, *Johnson Matthey Technol. Rev.*, 2024, **68**, (4), 477
88. M. Al Salmi, *Johnson Matthey Technol. Rev.*, 2024, **68**, (4), 490

The Author



Mustafa Al Salmi is a Production Engineer at Petroleum Development Oman (PDO). He received his BEng Chemical and Material Engineering from University of Leeds, UK, in 2021. He then completed his MSc Chemistry by Research from University of Lincoln, UK, and ISIS Neutron and Muon Source at the STFC Rutherford Appleton Laboratory near Oxford, UK between 2021 and 2023. His research expertise includes neutron vibrational spectroscopy techniques, first-principles computational modelling and data science to optimise chemical processes within the oil and gas industry. He also applies this knowledge to understand and predict heterogeneous catalysts and materials for use in sustainable chemical production, energy storage and pollution reduction. Additionally, his research background includes experience with various optimisation methods like differential evolution, particle swarm optimisation and simulated annealing, which he has employed to improve efficiency and performance in chemical engineering processes.
